The Intermediate Filament Protein Peripherin Is the Specific Interaction Partner of Mouse BPAG1-n (Dystonin) in Neurons

Conrad L. Leung,* Dongming Sun,‡ and Ronald K.H. Liem‡

*Departments of Biochemistry and Molecular Biophysics and ‡Departments of Pathology and Anatomy and Cell Biology, Columbia University College of Physicians and Surgeons, New York 10032

Abstract. The *dystonia musculorum* (*dt*) mouse suffers from severe degeneration of primary sensory neurons. The mutated gene product is named dystonin and is identical to the neuronal isoform of bullous pemphigoid antigen 1 (BPAG1-n). BPAG1-n contains an actin-binding domain at its NH_2 terminus and a putative intermediate filament-binding domain at its COOH terminus. Because the degenerating sensory neurons of *dt* mice display abnormal accumulations of intermediate filaments in the axons, BPAG1-n has been postulated to organize the neuronal cytoskeleton by interacting with both the neurofilament triplet proteins (NFTPs) and microfilaments. In this paper we show by a variety of methods that the COOH-terminal tail domain of mouse BPAG1 interacts specifically with peripherin, but in contrast to a previous study (Yang, Y., J. Dowling, Q.C. Yu, P. Kouklis, D.W. Cleveland, and E. Fuchs. 1996. *Cell.* 86:655–665), mouse BPAG1 fails to associate with full-length NFTPs. The tail domains interfered with the association of the NFTPs with BPAG1. In *dt* mice, peripherin is present in axonal swellings of degenerating sensory neurons in the dorsal root ganglia and is downregulated even in other neural regions, which have no obvious signs of pathology. Since peripherin and BPAG1-n also display similar expression patterns in the nervous system, we suggest that peripherin is the specific interaction partner of BPAG1-n in vivo.

Key words: BPAG1 • dystonin • peripherin • neurofilament • intermediate filament

INTERMEDIATE filaments (IFs)[1] are 10-nm filaments found in most eukaryotic cells and are made up of various IF proteins. Tissue-specific and developmental stage-specific expressions are intrinsic features of IF proteins. In the mammalian nervous system, five IF proteins are specifically expressed in differentiated neurons: the neurofilament (NF) triplet proteins (NF-L, NF-M, and NF-H), α-internexin, and peripherin (Fliegner and Liem, 1991; Ho and Liem, 1996; Lee and Cleveland, 1996). In the adult, the neurofilament triplet proteins (NFTPs) are widespread in the mature nervous system. They coassemble into heteropolymeric NFs and are especially abundant in neurons with large axons. α-Internexin and peripherin are more limited to small neurons, with α-internexin primarily in the central nervous system (CNS) and peripherin predominantly in the peripheral nervous system (PNS). During the development of the CNS, the expression of α-internexin precedes that of the NFTPs (Kaplan et al., 1990; Fliegner et al., 1994). For example, at embryonic day 12 (E12) in rat, α-internexin mRNA is readily detected in the basal forebrain where neurogenesis has just begun, whereas NF-L and NF-M are still minimal or absent (Fliegner et al., 1994). NF-H appears even later in development and its expression is very limited until after birth (Shaw and Weber, 1982; Pachter and Liem, 1984). Similar to α-internexin, peripherin is expressed early in development (Leonard et al., 1988; Parysek et al., 1988; Parysek and Goldman, 1988; Escurat et al., 1990; Troy et al., 1990a). As early as E9 in mouse and E12 in rat, peripherin can be detected in the PNS, e.g., in the dorsal root ganglia (DRG), cervical ventral roots, cranial nerve ganglia, and the enteric nervous system. The expression of peripherin continues through adulthood in the PNS. In adult rat, the expression of peripherin has also been observed in the CNS. For example, a subset of brainstem reticular formation was shown to be immunoreactive to a peripherin antiserum (Brody et al., 1989).

IFs are associated with a class of cytoskeletal cross-linking proteins, known as plakins or cytolinkers (Green et al.,

Address correspondence to Ronald K.H. Liem, Ph.D., Department of Pathology, Columbia University College of Physicians and Surgeons, 630 West 168th St., New York, NY 10032. Tel.: (212) 305-4078. Fax: (212) 305-5498. E-mail: RKL2@columbia.edu

1. *Abbreviations used in this paper:* BPAG1, bullous pemphigoid antigen 1; CNS, central nervous system; DRG, dorsal root ganglia; *dt*, *dystonia musculorum*; GAD, GAL4 activation domain; GBD, GAL4 DNA-binding domain; IF, intermediate filament; NF, neurofilament; NFTPs, neurofilament triplet proteins; nIF, neuronal IF; PNS, peripheral nervous system.

1992; Ruhrberg and Watt, 1997; Wiche, 1998). Five members of this family have so far been identified: desmoplakin, plectin, bullous pemphigoid antigen 1 (BPAG1), envoplakin, and periplakin (Bousquet and Coulombe, 1996; Ruhrberg et al., 1997; Fuchs and Cleveland, 1998; Houseweart and Cleveland, 1998; Wiche, 1998). Among these family members, BPAG1 and plectin have been reported to be expressed in neurons (Errante et al., 1994; Bernier et al., 1995; Dowling et al., 1997). BPAG1 was originally isolated as an autoimmunogen from patients with the skin disease bullous pemphigus and was later shown to be a 230-kD hemidesmosomal protein (Stanley et al., 1988; Mueller et al., 1989; Stanley, 1993; Lieber and Evans, 1996). Three alternatively spliced isoforms of BPAG1 have been fully characterized: one epidermal isoform (BAPG1-e) and two neuronal isoforms (BPAG1-n) (Brown et al., 1995a,b). Similar to the other members of the plakin/cytolinker family, BPAG1 exhibits a three-domain structure, consisting of a central rod domain flanked by NH_2-terminal head and COOH-terminal tail domains (Ruhrberg and Watt, 1997). The majority of the rod domain is composed of heptad repeats that mediate coiled–coil dimer formation. However, it is not known whether higher order structures can be formed. The NH_2-terminal head domain consists of six α-helical segments, whereas the COOH-terminal tail domain is made up of two homologous subdomains, known as the B and C domains (Green et al., 1992). The COOH-terminal tail domain has been suggested to interact with cytokeratins and NFs (Guo et al., 1995; Dowling et al., 1996; Yang et al., 1996). In addition, both of the neuronal isoforms of BPAG1 contain putative actin-binding domains at the ends of their NH_2 termini (Brown et al., 1995a).

Unlike plectin which is expressed only in a small subset of motoneurons (Errante et al., 1994), BPAG1-n is widespread in sensory neurons of adult mice, such as those in the DRG and cranial nerve ganglia (Bernier et al., 1995; Dowling et al., 1997). In addition, BPAG1-n is also present in neurons of the sympathetic nervous system, the enteric nervous system, and the cerebellum (Dowling et al., 1997). These expression patterns are similar to that of peripherin (Parysek et al., 1988; Troy et al., 1990a). During the development of the nervous system, BPAG1-n can be detected as early as E9.5 in differentiated neurons of mouse embryos (Dowling et al., 1997), coinciding with the expression of α-internexin and peripherin, but apparently is expressed before the NFTPs. The embryonic expression of BPAG1-n is not restricted to the developing sensory neurons; it is also detected in motoneurons. The importance of BPAG1 to maintain the integrity of the nervous system has been elucidated by knockout studies of the BPAG1 gene in transgenic mice (Guo et al., 1995) and by studies of natural mouse mutants with the neurological disorder, *dystonia musculorum* (*dt*). Mice carrying mutations in the BPAG1 gene, as a consequence of spontaneous mutations or gene targeting, develop dystonic movement, hyperextension, and hyperflexion of the limbs, and often die before weaning (Duchen et al., 1963; Duchen and Strich, 1964; Duchen, 1976; Guo et al., 1995). As a result, BPAG1-n is also known as dystonin. Histopathological studies revealed that *dt* mice and BPAG1−/− mice suffer from severe degeneration of primary sensory neurons. This pathology is especially prominent in the DRG, where degenerating neurons display abnormal accumulations of IFs in the axons (Duchen and Strich, 1964; Janota, 1972; Sotelo and Guenet, 1988; al-Ali and al-Zuhair, 1989; Guo et al., 1995). A recent study indicated that the COOH-terminal tail domain of BPAG1 colocalized with NF-L/NF-H heteropolymeric filaments in transiently transfected cells and coimmunoprecipitated with overexpressed NF-H proteins (Yang et al., 1996). Furthermore, full-length BPAG1-n protein coaligned with some of the filaments formed by the transfected NF-L and NF-H and the endogenous stress fibers in transfected cells. These studies led to the hypothesis that BPAG1-n is a cytoskeletal cross-linking protein, connecting NFs to microfilaments, and its functional perturbation causes NF disorganization that ultimately leads to neuronal degeneration (Brown et al., 1995a; Yang et al., 1996). However, the distribution pattern of BPAG1-n is much more restricted in the nervous system as compared with the NFTPs. This difference led to the question of whether BPAG1-n might interact with other neuronal IFs (nIFs). Therefore, we investigated the interactions of this protein with all of the nIFs. Surprisingly, we observed that the tail domain of BPAG1 associated with α-internexin and peripherin filaments, but not with filaments formed by full-length NFTPs.

Materials and Methods

Plasmid Construction

cDNAs of mouse BPAG1 COOH-terminal domain (mBPAG-C1) were synthesized by RT-PCR based on the original partial mouse BPAG1 sequence (Amagai et al., 1990). In brief, 1 μg of poly(A)$^+$ RNA from mouse brain (Clontech) was primed with random hexamers and reverse-transcribed with Moloney murine leukemia virus reverse transcriptase according to the manufacturer's protocol (Perkin Elmer). Three pairs of primers were used to amplify three consecutive overlapping fragments of the mBPAG-C1 cDNA. The first pair of primers included sense primer 5′-AAAACCTAGTAAGCGAGTTCAAGC-3′ and antisense primer 5′-TTTAAGGTCGTGACTTCTGTATGC-3′; the second pair of primers included sense primer 5′-AAGCTTTTGACACCCTTAGAGATA-3′ and antisense primer 5′-GAAAGTCAGCCAGTTCTGTTAGTG-3′; and the third pair of primers included sense primer 5′-CAGGAAGGCCTAACTACACTAACA-3′ and antisense primer 5′-TCTGCACAGAGTCAAACGCCCTAC-3′. The last antisense primer covers the termination codon of BPAG1. The three amplified fragments were subcloned into the pGEM-T vectors (Promega) and sequenced to confirm their identities. Unique restriction enzyme recognition sites, HindIII and StuI, at the overlapping regions were used to reconstruct the mBPAG-C1 cDNA. To generate pcDNA-FLAG-mBPAG-C1, the recovered mBPAG-C1 cDNA was ligated in frame to the 3′ end of the FLAG epitope tag sequence in a pcDNA3 (Invitrogen) derived expression vector. The original FLAG epitope tag-containing vector was a generous gift from Dr. Howard Worman (Columbia University, New York). To generate pcDNA-FLAG-mBPAG-C2, pTOPO-mBPAG-C2 was first made by cloning the PCR fragment of pcDNA-FLAG-mBPAG-C1 with sense primer 5′-GGCTTTTGATACGGCAGGGAG-3′ and antisense primer 5′-TCTGCACAGAGTCAAACGCCCTAC-3′ into the pCR2.1-TOPO vector (Invitrogen). The 2.3-kb EcoRI-EcoRV fragment of pTOPO-mBPAG-C2 was then ligated to the 5.4-kb fragment of EcoRI/EcoRV-digested pcDNA-FLAG-mBPAG-C1 to make pcDNA-FLAG-mBPAG-C2. All of the NFTPs, α-internexin, and peripherin expression constructs were cloned in the expression vector pRSVi and were described previously (Chin and Liem, 1989, 1990; Chin et al., 1991; Ching and Liem, 1993, 1998; Ho et al., 1995; Sun et al., 1997). To facilitate the coexpression of NF-L and NF-H in transiently transfected cells, a double expression construct, pCI-NFL/NFH, was created. pCI-NFL was first generated by cloning the blunt-ended 2.0-kb HindIII fragment from pRSVi-NFL into the SmaI site of pCI vector (Promega). pCI-NFH was then made by cloning

the 3.4-kb EcoRI fragment from pGBT-NFH into the EcoRI site of pCI vector (Promega). Afterwards, the 4.7-kb BamHI-BglII fragment of pCI-NFH, which contained the expression cassette of NFH, was isolated and ligated to the BamHI digested pCI-NFL to yield pCI-NFL/NFH.

Two-hybrid and three-hybrid constructs were made with plasmids pGBT9, pGAD424, pAS2-1, and pACT2 (Clontech). pGBT-mBPAG-C1 and pAS2-mBPAG-C1 were constructed by cloning the 3.0-kb EcoRV fragment of pcDNA-FLAG-mBPAG-C1 into the SmaI site of pGBT9 and pAS2-1, respectively. pGBT-mBPAG-r220 was engineered by removing the 2.2-kb BglII-BamHI fragment from pGBT-mBPAG-C1. All of the full-length and truncated NFTP two-hybrid constructs in pGAD424 have been described previously (Leung and Liem, 1996). To engineer pGAD-α-internexin, the NcoI(blunted)-BamHI fragment comprising the full-length α-internexin cDNA was isolated from pET-α-internexin and ligated to SmaI-BamHI–digested pGAD424. pGAD-Peri35-474 and pGBT-Peri35-474 were cloned by inserting the 1.8-kb SmaI-BamHI fragment of pRSVi-perM1M2 (Ho et al., 1995) into the SmaI-BamHI–digested pΔGAD424 and pΔGBT9 (Leung and Liem, 1996), respectively. To generate pACT-NFL24-542, pACT-NFM, and pACT-NFH, the HindIII fragments, containing the hybrids GAL4 activation domain (GAD)-fusion cDNA of pGAD-NFL24-542, pGAD-NFM, and pGAD-NFH, were cloned into the HindIII-digested pACT2 vector, respectively. To construct three-hybrid vector pGAD-NFL1-415/NFH1-415, pGAD-NFL1-415 was digested with SphI; and the 2.5-kb fragment containing the GAD-NFL1-415 expression cassette was then subcloned into the SphI partially digested pGAD-NFH1-415. Similar strategies were applied to create the other three-hybrid constructs, pGAD-NFL1-415/NFL1-415, pGAD-NFM1-421/NFM1-421, pGAD-NFH1-415/NFH1-415, and pGAD-NFL1-415/NFM1-421.

Prokaryotic expression constructs were made with plasmids, pET-3a, pET-3b, pET-16b, and pET-21d (Novagen). To create pET-mBPAG-C2, the 2.4-kb PCR fragment of pcDNA-FLAG-mBPAG-C2 with sense primer 5′-CCACCATGGACTACAAGGACGACG-3′ and antisense primer 5′-ACGGGATCCTGGGAAGAATAGTAGAGG-3′ was digested with BamHI and NcoI before being ligated to the BamHI-NcoI–digested pET-21d vector. To generate pET-NFL, NF-L cDNA in pGEM4 vector (Chin et al., 1989) was digested with SmaI and the purified insert was ligated to BamHI linkers before cloning into the BamHI site of pET-3b. Similarly, full-length NF-M cDNA (Napolitano et al., 1987) was digested with EcoRI; the insert was purified, blunt-ended, and ligated to BamHI linkers. The BamHI-linkered NF-M cDNA was then cloned into BamHI-digested pET-3a to make pET-NFM. For pET-NFH, the first ATG of NF-H cDNA was first mutagenized to an NdeI site. The NdeI-BamHI NF-H fragment was then purified and cloned into NdeI-BamHI–digested pET-3a. To engineer pET-peripherin, the 1.8-kb BamHI-SmaI fragment of pRSVi-perM1M2 (Ho et al., 1995) was ligated to 8-mer BamHI linkers, digested with BamHI, and cloned into the BamHI site of pET-16b vector.

Transient Transfections, Indirect Immunofluorescence Microscopy, and Confocal Microscopy

The SW13.cl.2Vim$^-$ cell line was grown at 37°C and 5% CO_2 in Dulbecco's modified Eagle's/Ham's F12 medium (Life Technologies, Inc.) supplemented with 5% fetal bovine serum. Transient transfection experiments were done by the calcium phosphate precipitation method as described previously (Sun et al., 1997). 48 h after transfection, coverslips with adherent cells were fixed in cold methanol at −20°C, washed several times with PBS, and incubated with primary antibodies at room temperature for 1 h. The primary antibody–treated cells were then washed with PBS and incubated with appropriate secondary antibodies for 30 min. Subsequently, the coverslips were washed with PBS and mounted onto slides with Aquamount (Lerner Laboratories) for immunofluorescent microscopy. Confocal microscopy was performed with an LSM 410 laser scanning confocal microscope (Zeiss), equipped with a krypton-argon laser, and attached to a Zeiss Axiovert 100 TV inverted fluorescence microscope. Usually, 20 optical sections were taken at 0.5-μm intervals. Images of 512 × 512 pixels were obtained, processed using Adobe Photoshop 3.0.

Yeast Transformation and β-Galactosidase Assays

Yeast strains SFY526 (*MATα, ura3-52, his3-200, ade 2-101, lys2-801, trp1-901, leu2-3, 112, can^r, gal4-542, gal80-538, URA3::GAL1-lazZ*) and HF7c (*MATα, ura3-52, his3-200, ade 2-101, lys2-801, trp1-901, leu2-3, 112, gal4-542, gal80-538, LYS2::GAL1-HIS3, URA3::(GAL4 17-mers)$_3$-CYC1-lazZ*) were grown and manipulated according to the MATCHMAKER two-hybrid system protocol (Clontech). In brief, the two-hybrid analysis was performed by cotransforming vectors in pairwise combinations into the SFY526 by the lithium acetate method, and the transformants were selected on minus Trp-Leu synthetic dropout plates for 4 d at 30°C. Filter lift assays were performed for the qualitative measurement of β-galactosidase activity as described (Leung and Liem, 1996). To carry out three-hybrid assays, two GAD-fusion vectors and one GAL4 DNA-binding domain (GBD)-fusion vector were transformed into yeast strain HF7c. The amount of GAD-fusion vectors used in each triple transformation was 20 times more than the normal amount used for double transformations. The triple transformants were selected on minus Trp-Leu-His synthetic dropout plates with 20 mM 3-aminotriazole for 7 d at 30°C. Liquid culture β-galactosidase assays with the substrate red-β-D-galactopyranoside (CPRG) were used for quantitative measurement of interactions and performed according to the MATCHMAKER Library Protocol PT1020-1 (Clontech). Yeast transformants were grown to mid-log phase and permeabilized by two freeze–thaw cycles in liquid nitrogen. Yeast extracts were then incubated with 2.23 mM CPRG solution. After the reaction mixtures started to change color, 3.0 mM $ZnCl_2$ was added to stop the reaction and OD_{578} was measured for calculation of β-galactosidase activity. A β-galactosidase unit is defined as $10^3 \times OD_{578}$/min of reaction for 1 ml of culture at 1 OD_{600} unit.

Protein Purification and Overlay Binding Assays

His-tagged FLAG-mBPAG-C2 and peripherin were solubilized in 8 M urea and purified on Ni^{2+} columns according to the pET system manual (Novagen). Bacterially expressed NFTPs were solubilized in 8 M urea and purified by hydroxylapatite chromatography as previously described (Liem and Hutchison, 1982). Purified FLAG-mBPAG-C2-His was dialyzed overnight in PBS before use. To perform the protein overlay assays, equal amounts (20 pmol) of purified IF proteins were subjected to SDS-PAGE and electrotransferred onto a nylon membrane (Millipore). The membrane was blocked overnight with 5% BSA in PBS containing 0.05% Tween 20, and incubated with 50 μg of purified FLAG-mBPAG-C2-His in 5 ml PBS/Tween 20 (0.05%) for 1 h. To visualize the bound FLAG-mBPAG-C2-His, the membrane was washed extensively with PBS/Tween 20 (0.05%), incubated with anti-FLAG mAb, washed with PBS/Tween 20 (0.05%), treated with HRP-conjugated goat anti–mouse IgG, and processed for chemiluminescence (ECL) according to the manufacturer's protocol (Amersham). To perform the slot-blot overlay assays, equal amounts of IF proteins (15 μmol) solubilized in 8 M urea were polymerized in vitro by overnight dialysis against PBS (pH 6.8). The polymerized IF proteins were then blotted onto a nitrocellulose membrane in a slot-blot apparatus (Schleicher & Schuell). After blocking by 5% BSA, the blot was incubated with FLAG-mBPAG-C2-His. After extensive washing, the bound FLAG-mBPAG-C2-His was detected by blotting with anti-FLAG mAb as described above. The relative amounts of bound FLAG-mBPAG-C2-His were determined by scanning the autoradiograph and quantifying using the NIH Image 1.61 program.

Mouse Strains, Immunohistochemistry, and Western Blot Analysis

Heterozygote breeders of dystonia mouse strain B6CFe-*a/a-dt^l* were purchased from The Jackson Laboratory and homozygote offspring were identified phenotypically. Standard procedures for preparing samples for cryosectioning and immunostaining were performed. Spinal cords with attached DRG were dissected from perfused mice, postfixed in 4% paraformaldehyde for 4 h, and incubated in 20% sucrose solution overnight. 15-μm sections were cut and placed on gelatin-coated slides. The tissues were then fixed with −20°C methanol, blocked with 5% normal goat serum, and incubated with mouse monoclonal antiperipherin antibody. Diaminobenzidine/peroxidase immunostaining with HRP-conjugated secondary antibody was then carried out to detect peripherin in the tissues. To collect samples for Western blots, anatomical structures were dissected out of killed mice and homogenized in lysis buffer containing 6.25 mM Tris-HCl (pH 7.5), 1% SDS, 5 mM EDTA, and a cocktail of protease inhibitors. Standard procedures for SDS-PAGE, protein transfer to nylon membranes, immunostaining, and chemiluminescence (ECL; Amersham Life Sciences) were used.

Antibodies

The following primary antibodies were used for immunofluorescence staining, immunohistochemistry, and Western blots: mouse anti-FLAG M2 mAb (IBI-Kodak); rabbit polyclonal anti–α-internexin AbαNcoA antibody and mouse anti–α-internexin mAB135 mAb (Kaplan et al., 1990); rabbit polyclonal antiperipherin Ab6264 antibody (Aletta et al., 1988) and mouse antiperipherin mAb (Chemicon); rabbit polyclonal antivimentin antibody (a gift from Dr. Eugenia Wang, Lady Davis Institute for Medical Research, Montreal, Canada); mouse anti-NFL NR4 mAb (Sigma); and rabbit polyclonal antibodies against NF-L (Kaplan et al., 1991).

Results

Isolation of a cDNA Clone Encoding the Mouse BPAG1 COOH-terminal Domain

To study the interactions of BPAG1 with nIFs, we isolated three consecutive overlapping pieces of the BPAG1 cDNA by RT-PCR on mouse brain mRNA. The three amplified DNA fragments were ligated together to yield a ~3.0-kb partial mouse BPAG1 cDNA. Sequencing of this cDNA showed that it encoded 988 amino acids, including the entire tail domain (768 amino acids) and the COOH terminus of the rod domain (220 amino acids). Because the complete mouse BPAG1 cDNA sequence had not been fully characterized (Amagai et al., 1990), the nomenclature of the mouse BPAG1 COOH-terminal proteins was designated according to the sequence of the human BPAG1 epidermal isoform (Fig. 1). We compared our sequence with several EST clones using BLAST. The sequences of a series of I.M.A.G.E. clones (clones 1262090, 931676, 1227492, 1242939, 975299, 317229, and 975617) are identical to the sequence of mBPAG-C2 and cover 75% of the sequence. Furthermore, the mBPAG-C1 sequence is identical to the deduced protein sequence of BPM1, a partial mouse BPAG1 cDNA (accession number 321215; Amagai et al., 1990). The accession number for the mouse BPAG-C1 sequence is AF115383.

As deduced from the respective cDNA sequences, the amino acid composition of the mouse BPAG1 tail domain is ~80% identical to that of the human BPAG1 tail domain. Similar to the human orthologue, the tail domain of mouse BPAG1 contains two homologous subdomains, B and C.

Mouse BPAG1 COOH-terminal Protein Associates with α-Internexin and Peripherin, but Not with NFTPs in the Yeast Two-Hybrid System

A recent study on the interactions of desmoplakin with cytokeratins indicated that the yeast two-hybrid system is a useful tool to characterize associations between plakins/cytolinkers and IF proteins (Meng et al., 1997). Therefore, we initially studied the associations of mBPAG-C1 with nIF proteins by a similar approach. mBPAG-C1 was fused with the GBD in vector pGBT9 (Fig. 1), and was tested in pairwise combinations with various GAD-fused nIF proteins that were expressed by the pGAD424 vector. Interactions between mBPAG-C1 and nIF proteins were determined by qualitative β-galactosidase filter lift assays of the yeast cotransformants. Surprisingly, mBPAG-C1 interacted with α-internexin and peripherin, but not with vimentin, NF-L, NF-M, or NF-H in the two-hybrid studies (Table I). To determine whether the last 220 amino acids of the mouse BPAG1 rod domain in mBPAG-C1 interact nonspecifically with the IF proteins in the two-hybrid system, we also prepared GBD-mBPAG-r220 and tested for its binding with each of the GAD-nIFs. No interactions between GBD-mBPAG-r220 and any one of the GAD-nIFs were observed (Table I). Because the expression levels of fusion proteins might play a role in detecting weak interactions, we also cloned cDNAs of mBPAG-C1 and each of the NFTPs into higher expression two-hybrid shuttle vectors, pAS2-1 and pACT2, and reexamined their interactions. However, we were still not able to detect any interactions between mBPAG-C1 and any of the NFTPs (Table I).

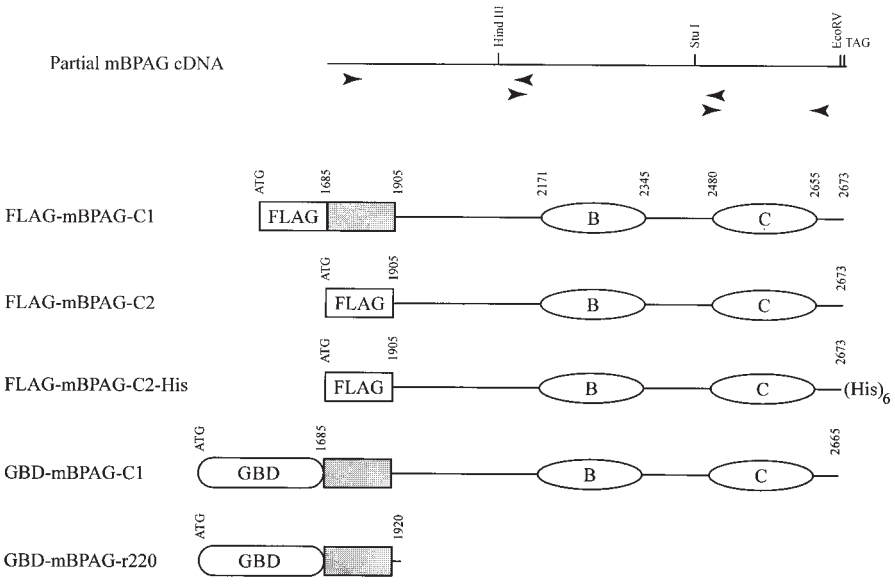

Figure 1. Schematic representation of the mouse BPAG1 COOH-terminal proteins. The top line corresponds to the partial mouse BPAG1 cDNA with the restriction sites used in this study. The arrows underneath this line denote the primers used for RT-PCR. Diagrammatic representations of FLAG-tagged BPAG1 COOH-terminal proteins used for transient transfection assays and GBD-fused mBPAG-C1 and mBPAG-r220 used for two-hybrid studies are shown. The numbers of the amino acids are assigned according to the human BPAG1-e sequence. Compared with that of the human orthologue, the tail domain of mouse BPAG1 has an extra glutamine before the stop codon. B and C stand for the B and C subdomains of BPAG1, respectively. The shaded box symbolizes the COOH terminus of the mouse BPAG1 rod domain.

Table I. Two-Hybrid Analysis of the Interactions between GBD-mBPAG1 Proteins and nIF Proteins

	mBPAG-C1	mBPAG-r220
NF-L	−	−
NF-M	−	−
NF-H	−	−
α-Internexin	+	−
Peripherin	+	−
Vimentin	−	−

SFY526 cells cotransformed with pGBT-mBPAG-C1 or pGBT-mBPAG-r220 and various pGAD-nIFs were selected in minus Trp-Leu media. The plus and minus signs represent the results of the β-galactosidase filter lift assays on cotransformants. The NF-L and peripherin constructs code for amino acids 24–542 of NF-L and amino acids 35–474 of peripherin, respectively. In the case of NFTPs studies, identical results were obtained from GAD-fused NFTPs expressed by vector pACT2 and GBD-fused mBPAG-C1 expressed by vector pAS2-1.

Mouse BPAG1 COOH-terminal Proteins Colocalize with α-Internexin and Peripherin Filaments, but Not with NFTP Filaments in Transiently Transfected Cells

The results of the two-hybrid experiments prompted us to repeat some of the transient transfection assays performed by Yang et al. (1996) on mBPAG-C1 and NFTPs. In addition, we wanted to confirm the interactions of mBPAG-C1 with α-internexin and peripherin. To facilitate the detection of mBPAG-C1 in the transient transfection assays, the NH_2 terminus of mBPAG-C1 was fused to a FLAG epitope tag, which also provided the translational start codon (Fig. 1). All transfections were performed in a human adrenal carcinoma cell line, SW13.cl.2Vim$^-$, because it did not contain any cytoplasmic IFs that might interact with mBPAG-C1. Cotransfections of mBPAG-C1 with peripherin showed colocalization of mBPAG-C1 with peripherin filament networks in transiently transfected cells (Fig. 2, A and B). In contrast, mBPAG-C1 appeared to disrupt the normal filament formation of α-internexin. α-Internexin has been shown previously to self-assemble into normal filamentous networks in transiently transfected SW13.cl.2Vim$^-$ cells (Fig. 2 F; Ching and Liem, 1993). In the presence of mBPAG-C1, the filaments formed by α-internexin became bundled and these bundles were decorated with mBPAG-C1 (Fig. 2, D and E). In addition, the punctate background staining patterns observed with both antibodies suggest that interaction with mBPAG-C1 prevented some α-internexin molecules from self-assembly into filaments. Although mBPAG-C1 did not colocalize with vimentin filaments in transfected cells, it seemed to have some influence on the morphology of the assembled vimentin filament network (Fig. 2, G–I). Since none of the NFTP subunits can self-assemble into filamentous networks (Ching and Liem, 1993; Lee et al., 1993), transient transfections of mBPAG-C1 with NF-L and NF-M or with NF-L and NF-H were performed in order to detect potential interactions between BPAG1-n and polymerized NFs. In contrast to a previous report (Yang et al., 1996), we did not observe any colocalization between mBPAG-C1 and the filament networks formed by NF-L and NF-M or by NF-L and NF-H. Instead, the immunostaining pattern of mBPAG-C1 was diffuse in the presence of these filament networks in the transfected SW13.cl.2Vim$^-$ cells (Fig. 3). To verify that these patterns

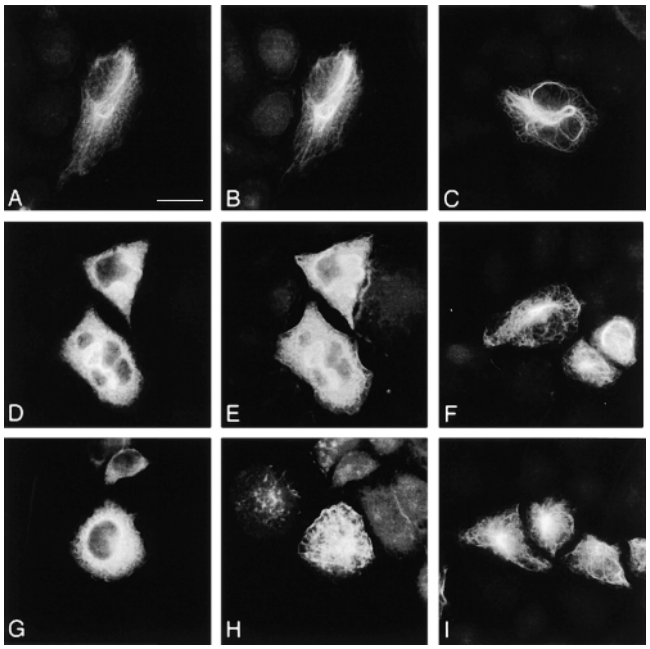

Figure 2. Analysis of mBPAG-C1 with peripherin, α-internexin, and vimentin filament networks in transient transfection studies. SW13.cl.2Vim$^-$ cells from transient transfections of pRSVi-peripherin (C), pRSVi-α-internexin (F), or pRSVi-vimentin (I), and cotransfections of pcDNA-FLAG-mBPAG-C1 with (A and B) pRSVi-peripherin, (D and E) pRSVi-α-internexin, or (G and H) pRSVi-vimentin were double-labeled with mouse anti-FLAG M2 mAb (A, D, and G) and rabbit polyclonal antibodies against peripherin (B and C), α-internexin (E and F), or vimentin (H and I). mBPAG-C1 associated with the filament network of peripherin, but disrupted the normal filament network of α-internexin. The perturbed α-internexin filament bundles were decorated with mBPAG-C1. The expressed mBPAG-C1 also appeared to affect the morphology of the vimentin filament network. Bar, 10 μm.

were indeed distinct, we performed confocal microscopy on the cells cotransfected with mBPAG-C1, NF-L, and NF-H. As shown in Fig. 3, C and D, the filamentous staining pattern observed for NF-L/NF-H filaments did not colocalize with the diffuse mBPAG-C1 staining pattern.

The discrepancy between our results and Yang et al. (1996) could be due to the presence of the partial rod domain in our mBPAG-C1 protein. To investigate this possibility, transient transfections with pcDNA-FLAG-mBPAG-C2 construct were carried out. mBPAG-C2 contains only the mouse BPAG1 tail domain (Fig. 1) and is therefore the mouse equivalent of the human BPAG1 tail domain used by Yang et al. (1996). As shown in Fig. 4 by confocal microscopy, mBPAG-C2 also colocalized with the peripherin filament network, but not with the NF-L/NF-H filament network. Moreover, mBPAG-C2 disrupted the α-internexin filament network and showed no correlation with the NF-L/NF-M filament network (data not shown). Because identical results were obtained by using either mBPAG-C1 or mBPAG-C2, we concluded that the presence of the partial rod domain in mBPAG-C1 did not

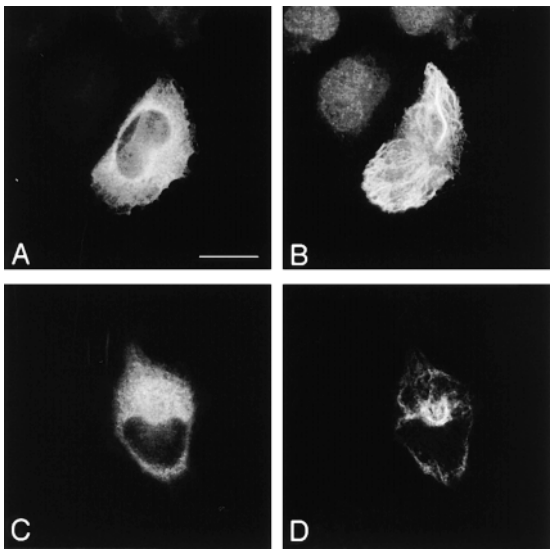

Figure 3. mBPAG-C1 did not associate with the filamentous networks formed by NF-L/NF-M or NF-L/NF-H in transiently transfected cells. Transient transfections of pcDNA-FLAG-mBPAG-C1 with pRSVi-NF-L and pRSVi-NF-M (A and B) or with pCI-NFL/NFH (C and D) were performed in SW13.cl.2Vim$^-$ cells. Transfected cells were stained with mouse anti-FLAG M2 mAb (A and C) and rabbit polyclonal antibody against NF-L (B and D), and examined by regular immunofluorescence microscopy (A and B) or confocal microscopy (C and D). In the presence of NF-M or NF-H, NF-L was able to form filamentous networks, but mBPAG-C1 failed to colocalize with these filaments. Bar, 10 μm.

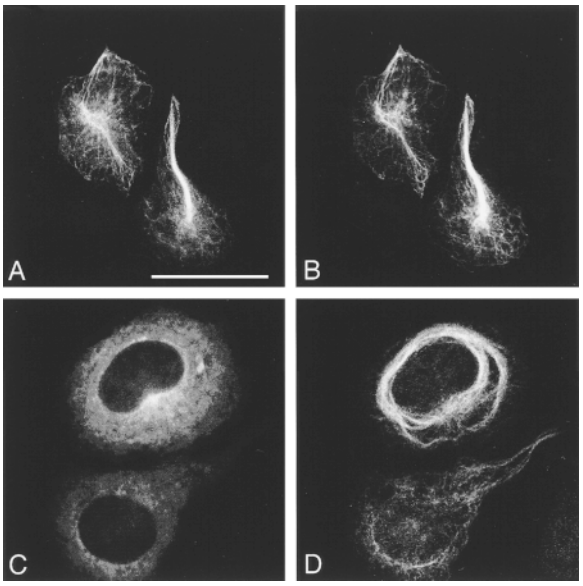

Figure 4. mBPAG-C2 associated with peripherin filaments but not with NF-L/NF-H filaments in transiently transfected cells. Transient transfections of pcDNA-FLAG-mBPAG-C2 with pRSVi-peripherin (A and B) or with pCI-NFL/NFH (C and D) were performed in SW13.cl.2Vim$^-$ cells. Transfected cells were stained with mouse anti-FLAG M2 mAb (A and C), rabbit polyclonal antibodies against peripherin (B), and rabbit polyclonal antibody against NF-L (D), and were examined by confocal microscopy. Similar to mBPAG-C1, mBPAG-C2 only colocalized with peripherin filaments and showed no correlation with the NF-L/NF-H filaments. Bar, 10 μm.

affect its interaction with IF networks in transient transfection assays.

Mouse BPAG-C2 Interacts with Peripherin, but Not with NFTPs in Overlay Binding Assays

To confirm the specificity of the interaction between mBPAG-C2 and peripherin, we also used in vitro overlay binding assays. Peripherin was chosen, instead of α-internexin, because its in vivo expression pattern resembles that of BPAG1-n; therefore, their interaction is of more physiological significance (Parysek and Goldman, 1988; Troy et al., 1990a; Dowling et al., 1997). Recent studies on the interactions of plectin and desmoplakin with IF proteins demonstrated that the association between these proteins can be monitored by overlay binding assays (Nikolic et al., 1996; Meng et al., 1997). Hence, we examined the interactions between mBPAG-C2 and IF proteins by similar strategies. Bacterially expressed IF proteins and mBPAG-C2 were successfully purified by column chromatography (Fig. 5 A). Purified IF proteins were resolved by SDS-PAGE and transferred onto a nylon membrane. After the removal of SDS by washing in PBS (0.05% Tween 20 and 5% BSA), the membrane was incubated with mBPAG-C2 protein. The bound mBPAG-C2 was detected by an anti-FLAG mAb. As illustrated in Fig. 5 B, mBPAG-C2 associated with peripherin protein, but not with the NFTPs.

Since it is possible that the interaction of mBPAG-C2 and NFs occurs only with polymerized IFs, we reassembled peripherin, as well as combinations of NF-L/NF-M and NF-L/NF-H, in vitro by dialysis against PBS. The reassembled filaments were then examined for possible interactions with mBPAG-C2 using a slot-blot overlay assay. The relative amounts of mBPAG-C2 bound to the various polymerized IFs were measured by densitometric analysis. As shown in Fig. 5 C, the BPAG1 tail domain interacted with polymerized peripherin, but not with polymerized NF-L/NF-M or NF-L/NF-H.

Mouse BPAG-C1 Interacts with Tailless NFTPs in the Two-Hybrid Assays

Since we have shown that NF-H and NF-M prefer to form heterodimers with NF-L (Leung and Liem, 1996), we performed three-hybrid studies to examine whether mBPAG-C1 could associate with heterodimers of NF-L/NF-M (L/M) or NF-L/NF-H (L/H). We took advantage of the yeast strain HF7c, which contained a *HIS3* reporter gene, as well as a weak lacZ reporter gene. We reasoned that if mBPAG-C1 could interact with heterodimers of L/M or L/H, triple transformants of pGBT-mBPAG-C1/pGAD-NFL/pGAD-NFM or pGBT-mBPAG-C1/pGAD-NFL/pGAD-NFH in HF7c would grow on minus histidine-leucine-tryptophan synthetic dropout plates. In addition, the selective pressure of histidine-free medium would keep all three plasmids in the same cells, provided that the expressed proteins interacted together as a unit. Under these conditions, there were still no interactions between

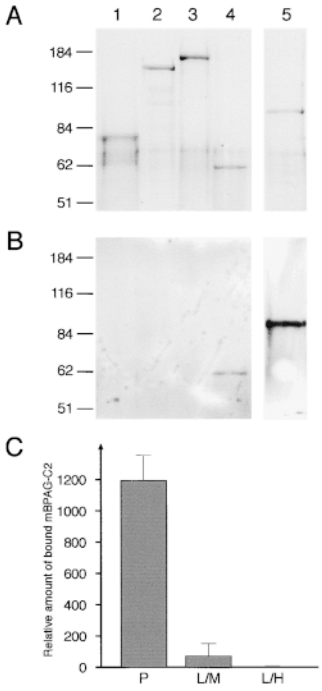

Figure 5. Specific interactions of mBPAG-C2 with peripherin in overlay binding assays. (A) Coomassie brilliant blue staining of purified NF-L (lane 1), NF-M (lane 2), NF-H (lane 3), peripherin (lane 4), and FLAG-mBPAG-C2-His (lane 5). (B) Equal amounts of NF-L (lane 1), NF-M (lane 2), NF-H (lane 3), and peripherin (lane 4) were subjected to SDS-PAGE and electrotransferred onto a nylon membrane. The membrane containing the nIF proteins was incubated with FLAG-mBPAG-C2-His and the bound FLAG-BPAG-C2-His was visualized by immunoblotting with monoclonal anti-FLAG M2 antibody. Lane 5 is a Western blot of FLAG-mBPAG-C2-His detected by the anti-FLAG antibody. (C) Peripherin (P), NF-L/NF-M (L/M), and NF-L/NF-H (L/H) were polymerized in vitro, dotted onto a nitrocellulose membrane, and incubated with FLAG-mBPAG-C2-His. Bound FLAG-mBPAG-C2-His was visualized with the anti-FLAG M2 antibody and quantified as described. Data shown are averages of triplicate determinations.

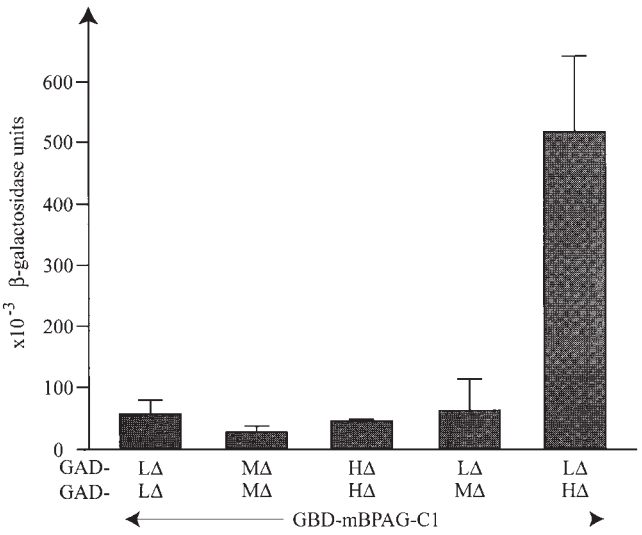

Figure 6. Three-hybrid analysis of interactions between mBPAG-C1 and NFTPs. Three-hybrid vectors containing two expression cassettes of GAL4 transactivation domain fused to NFTPs were cotransformed with pGBT-mBPAG-C1 in SFY526 yeast cells. Cells were grown to mid-log phase in minus Trp-Leu media and permeabilized for quantitative β-galactosidase assays as described in the text. LΔ, MΔ, and HΔ refer to the tailless proteins NFL1-415, NFM1-421, and NFH1-415, respectively.

mBPAG-C1 and L/M or L/H (Table II). Therefore, we postulated that the failure of NFTPs to interact with mBPAG-C1 might be inherent in the structure of the molecules. Since the greatest differences among nIF proteins are at their tail domains, we prepared tailless NFTPs (LΔ, MΔ, and HΔ) and tested for their interactions with mBPAG-C1 in yeast strain HF7c. We observed fast growing colonies in triple transformants of pGBT-mBPAG-C1/pGAD-LΔ/pGAD-HΔ. Some of these colonies also displayed weak β-galactosidase activities. These results imply that mBPAG-C1 interacted with heterodimers of tailless NF-L and NF-H (Table II). However, this interpretation was tempered, because very slow growing small colonies were also detected in cotransformants of pGBT-mBPAG-C1 with any one of the tailless GAD-NFTP fusion vectors, indicating weak interactions between the tailless NFTPs and mBPAG-C1 (Table II). To evaluate whether mBPAG-C1 really preferred to bind to the heterodimer of tailless NF-L and tailless NF-H, we constructed pGAD424-based three-hybrid vectors that contained two expression cassettes. By these means, two GAD fusion proteins could be expressed in the same transformant with single selection. Cotransformants of the three-hybrid vectors and pGBT-mBPAG-C1 would express the three fusion proteins simultaneously. Quantitative measurements of β-galactosidase activities were used to determine the relative strength of each interaction. The yeast transformants with pGBT-mBPAG-C1/pGAD-LΔ/pGAD-HΔ consistently displayed a high β-galactosidase activity, further confirming that mBPAG-C1 interact strongly with the LΔ/HΔ heterodimer (Fig. 6).

Table II. Two-Hybrid Interactions of mBPAG-C1 and NFTPs in the Yeast Strain HF7c

	GBD-mBPAG-C1									
GAD-	L	M	H	L + M	L + H	LΔ	MΔ	HΔ	LΔ + MΔ	LΔ + HΔ
HIS$^+$	−	−	−	−	−	SC	SC	SC	SC	SC + FC
LacZ$^+$	ND	ND	ND	ND	ND	−	−	−	−	+

HF7c cells cotransformed with pGBT-mBPAG-C1 and GAD-fused NFTPs constructs were selected in minus Trp-Leu-His media for 7 d. SC and FC correspond to the appearance of slow growing and fast growing colonies, respectively; minus sign, no colonies. β-Galactosidase filter lift assays were also performed for the growing colonies; plus and minus signs represented the results of the filter assays; ND, not determined. L, M, H, LΔ, MΔ, and HΔ refer to NFL24-542, NFM, NFH, NFL1-415, NFM1-421, and NFH1-415, respectively. GAD-NFL24-542, GAD-NFM, and GAD-NFH were expressed from the higher expression vector pACT2, whereas GAD-fused tailless NFTPs were expressed from pGAD424 vector.

Mouse BPAG-C1 Associates with Nonfilamentous Structures Formed by Tailless NFTPs in Transiently Transfected Cells

To determine if the tail domains of NFTPs also interfered with the association of mBPAG-C1 with filaments formed by NF-L/NF-M or NF-L/NF-H in the transient transfection assays, we performed cotransfections of mBPAG-C1 with various combinations of tailless and full-length NFTPs. As described previously, normal filament networks are observed from coassembly of tailless NF-L and wild-type NF-M or coassembly of wild-type NF-L and tailless NF-M in transiently transfected SW13.cl.2Vim$^-$ cells (Ching and Liem, 1993). However, mBPAG-C1 did not associate with any of the filamentous networks formed from these coas-

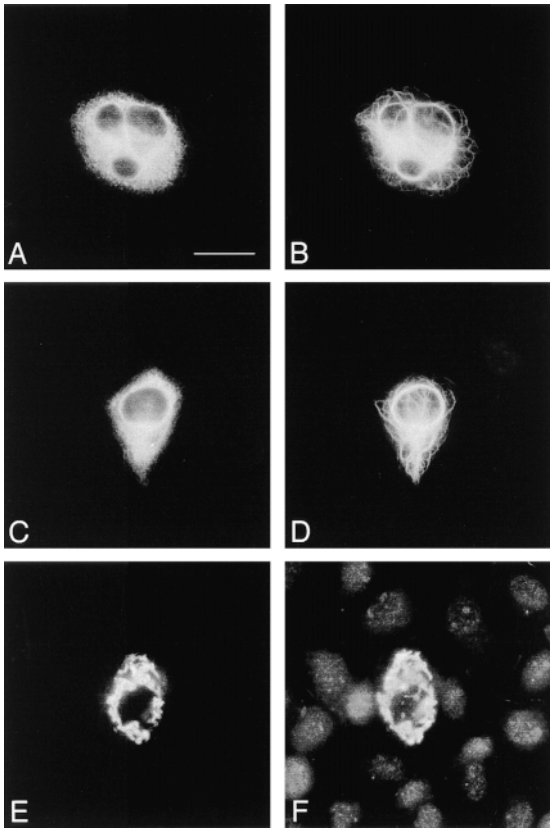

Figure 7. Interactions of mBPAG-C1 with aggregates of NF-L/NF-M proteins. SW13.cl.2Vim$^-$ cells from transient transfections of pcDNA-FLAG-mBPAG-C1 with (A and B) pRSVi-NFL1-415 and pRSVi-NFM; (C and D) pRSVi-NFL and pRSVi-NFM1-421; (E and F) pRSVi-NFL1-415 and pRSVi-NFM1-421 were double-labeled with mouse anti-FLAG M2 mAb (A, C, and E) and rabbit polyclonal antibody against NF-L (B, D, and F). A normal filament network could be formed by wild-type NF-L and tailless NF-M or by tailless NF-L and wild-type NF-M, but mBPAG-C1 did not colocalize with these filament networks. mBPAG-C1 only associated with the aggregates formed by tailless NF-L and tailless NF-M. Bar, 10 μm.

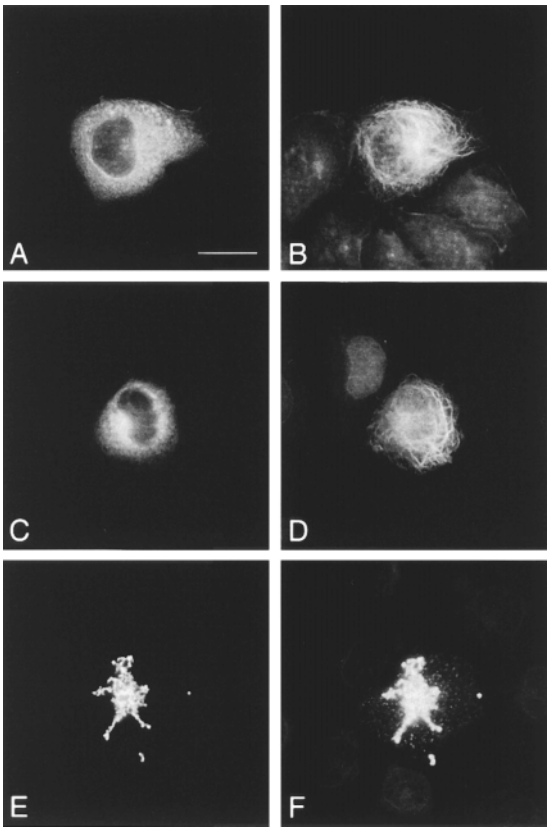

Figure 8. Interactions of mBPAG-C1 with aggregates of tailless NF-L/NF-H proteins. SW13.cl.2Vim$^-$ cells from transient triple-transfections of pcDNA-FLAG-mBPAG-C1 with (A and B) pRSVi-NFL1-415 and pRSVi-NFH; (C and D) pRSVi-NFL and pRSVi-NFH1-415; (E and F) pRSVi-NFL1-415 and pRSVi-NFH1-415 were double-labeled with mouse anti-FLAG M2 mAb (A, C, and E) and rabbit polyclonal antibody against NF-L (B, D, and F). mBPAG-C1 only associated with the aggregates formed by tailless NF-L and tailless NF-H. Bar, 10 μm.

semblies and maintained a diffuse staining pattern (Fig. 7, A–D). mBPAG-C1 only colocalized with aggregates formed by coassembly of tailless NF-L and tailless NF-M (Fig. 7, E and F). These results implied that the tail domains of NF-L and NF-M interfered with the binding of mBPAG-C1 to the filament networks formed by these proteins. When we transfected wild-type NF-H with tailless NF-L in SW13.cl.2Vim$^-$ cells, we observed filamentous staining as reported previously (Ching and Liem, 1993). However, mBPAG-C1 showed a diffuse staining pattern without any colocalization with the filaments formed by the tailless NF-L and wild-type NF-H (Fig. 8, A and B). Tailless NF-H formed filaments with wild-type NF-L (Sun et al., 1997), but the coexpressed mBPAG-C1 did not associate with this filament network (Fig. 8, C and D). In contrast, mBPAG-C1 was able to associate with the aggregates formed by tailless NF-L and tailless NF-H (Fig. 8, E and F). These experiments showed that the presence of any of the NFTP tail domains was sufficient to prevent NFTPs from interacting with mBPAG-C1.

Pathological Changes of Peripherin in dt Mice

Since the COOH-terminal domain of mouse BPAG1 is able to associate with peripherin and the two proteins share a similar in vivo expression pattern, we wanted to determine whether there was any peripherin involvement in the development of *dt* pathology. We first looked at the peripherin immunostaining in the DRG of *dt* mice and their normal littermates. As expected, peripherin was present in the axonal swellings of *dt* mice (Fig. 9). We then compared the amounts of various nIF proteins, actin, and tubulin in nervous tissues of 3-wk-old homozygous *dt* mice and their normal littermates. Although the amounts of NF-L, α-internexin, actin, and tubulin were similar between *dt* mice and their normal littermates, peripherin was generally downregulated in the *dt* mice (Fig. 10). The other two NFTPs, NF-M and NF-H, were present in comparable amounts between the homozygous *dt* mice and their normal littermates (data not shown). It should also be noted that the sciatic nerves of *dt* mice were smaller in diameter and yielded less protein than their normal littermates. These changes in the sciatic nerves are probably the result of the neuronal degeneration observed in *dt* mice.

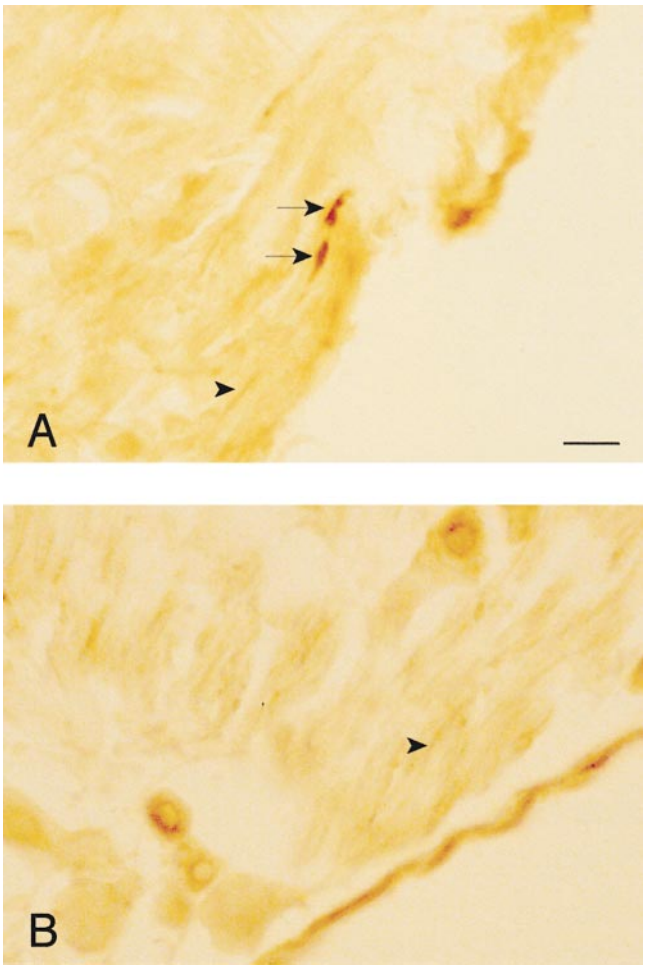

Figure 9. Peripherin can be detected in the axonal swellings of *dt* mice. Cryosections of the DRG from (A) *dt* mouse and (B) normal littermate were immunostained with peripherin mAbs. Arrows point to the peripherin staining in axonal swellings, whereas arrowheads point to peripherin staining in normal looking axons. Bar, 10 μm.

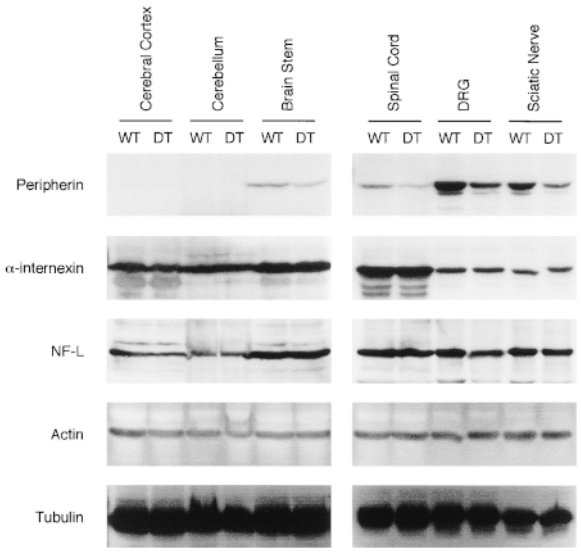

Figure 10. Peripherin is downregulated in nervous tissues from *dt* mice. Western blots of nervous tissues from *dt* mice (DT) and normal littermates (WT) were immunostained with various antibodies as indicated. Loadings of same amounts of total protein in each set of tissue samples from *dt* mice and normal littermates were confirmed by Ponceau red staining (data not shown). In the case of peripherin and NF-L immunostainings, the blots were first probed with antiperipherin antibody, and then were stripped and reprobed with anti-NFL antibody. The amounts of the protein samples on the blots immunostained with anti–α-internexin antibody were the same as those used for the NF-L and peripherin immunostainings, while one-half and one-third of the amounts were used for the blots immunostained with antiactin and antitubulin antibodies, respectively. 43–58% reduction of peripherin was detected in various nervous tissues of the *dt* mice as determined by densitometric analysis.

Discussion

Interactions of BPAG1 COOH-terminal with the NFTPs: Interference by the NFTP Tail Domains

The biochemical and cellular mechanisms underlying the neurological degeneration of *dt* mice have received a lot of attention recently in the IF field (Bousquet and Coulombe, 1996; Fuchs and Cleveland, 1998; Houseweart and Cleveland, 1998). The presence of an IF-binding domain in BPAG1 (dystonin), the mutated gene product, and the abnormal accumulations of NFs in the degenerating sensory neurons of the *dt* mice resulted in the hypothesis that BPAG1-n is an important organizing element of NFs in sensory neurons (Brown et al., 1995a; Yang et al., 1996). Our studies have demonstrated that the IF-binding tail domain of mouse BPAG1 does not interact with full-length NFTPs. This finding poses a disparity with a recent study which showed that the tail domain of human BPAG1-n associated with the heteropolymeric filaments formed by murine NF-L and NF-H in transiently transfected SW13.cl.2Vim$^-$ cells (Yang et al., 1996). We did not observe any colocalization of mouse BPAG1 COOH-terminal proteins with the filaments formed by rat NF-L and NF-H or by NF-L and NF-M. It should be noted that a similar FLAG-tag was used for the detection of the BPAG1 proteins in both studies. The three-hybrid assays and cotransfection experiments in our studies indicated that mBPAG-C1 interacted strongly with tailless NF-L and tailless NF-H, whereas the presence of the tail domains of any of the NFTPs appeared to prevent the assembled filaments from interacting with mBPAG-C1 (Table III). Yang et al. (1996) also showed that mouse NF-H protein overexpressed in COS cells was coimmunoprecipitated with the tail domain of human BPAG1-n, suggesting a direct interaction between NF-H protein and BPAG1-n. However, in our two-hybrid studies and overlay analysis, no interactions were detected between the BPAG1 COOH-terminal proteins and full-length NF-H. This discrepancy could be due to the presence of other IF proteins in the COS cells, which might serve as mediators between BPAG1 and NF-H. To circumvent this possibility, we repeated the immunoprecipitation experiments by using the SW13.cl.2Vim$^-$ cell line that is devoid of cytoplasmic IFs, but were not able to observe the coimmunoprecipitation of

Table III. Summary of Transient Transfection Studies on BPAG1 COOH-terminal Proteins and nIFs

Transfection	IF phenotype	BPAG colocalization
BPAG/vimentin	Filaments	No
BPAG/α-internexin	Filament bundles, punctate	Yes
BPAG/peripherin	Filaments	Yes
BPAG/L/M	Filaments	No
BPAG/L/H	Filaments	No
BPAG/L1-421/M	Filaments	No
BPAG/M1-415/L	Filaments	No
BPAG/L1-421/M1-415	Aggregates	Yes
BPAG/L1-421/H	Filaments	No
BPAG/H1-415/L	Filaments	No
BPAG/L1-421/H1-415	Aggregates	Yes

mBPAG-C1 with NF-H, either in the presence or absence of NF-L. We are at a loss to explain the discrepancies of our experiments with those described by Yang et al. (1996). The only difference between our experiments is the source of BPAG1. Our COOH-terminal domain constructs were cloned from mouse brain mRNA, whereas the constructs made by Yang et al. (1996) were obtained from a human cDNA library. However, BPAG1 is highly conserved between human and mouse; the primary sequence is 80% identical.

Interactions of BPAG1 with Peripherin: Relationship to the Pathogenesis of the dt Mouse

Although we were unable to show interactions between BPAG1 COOH-terminal proteins and the full-length NFTPs, we clearly demonstrated that the COOH-terminal domain of BPAG1-n can associate with the other two nIFs, peripherin and α-internexin, in the yeast two-hybrid and cotransfection experiments (Tables I and III). The interaction of BPAG1 with peripherin is of particular interest, because the two proteins exhibit similar expression patterns in the mouse PNS (Parysek et al., 1988; Troy et al., 1990a; Bernier et al., 1995; Dowling et al., 1997). We confirmed these interactions by overlay binding assays. We tested interactions of the mouse BPAG1 tail domain with NFTPs and peripherin that had been separated by SDS-PAGE and transferred onto a nylon membrane, as well as with repolymerized filaments that had been immobilized on a nitrocellulose membrane. In both cases, specific interactions were observed only between peripherin and BPAG1. The strong and specific interactions between peripherin and BPAG1 in the two-hybrid and overlay binding assays, the colocalization of BPAG1 COOH-terminal proteins with peripherin filaments in transient transfection studies, and the similarity in their in vivo expression patterns strongly suggest that peripherin is an important interaction partner of BPAG1-n. We also performed preliminary studies on the pathological changes associated with peripherin in *dt* mice. Axonal swellings of sensory neurons in the DRG are the most significant histopathological hallmarks of *dt* mice (Duchen et al., 1963; Duchen and Strich, 1964; Sotelo and Guenet, 1988; al-Ali and al-Zuhair, 1989; Guo et al., 1995). Immunostaining with antiperipherin antibody in the DRG revealed its presence in these axonal swellings (Fig. 9), although not all swellings were immunoreactive to the peripherin antibodies (data not shown). At present, it is not clear whether peripherin is absent in some of these swellings or just too scarce to be detected immunohistochemically. We also observed a general downregulation of peripherin in *dt* mice. The reduction in the peripherin levels is not restricted to the PNS. It is also detected in the CNS (Fig. 10), although no overt structural abnormalities have been observed in the CNS (Duchen et al., 1963). Presumably, peripherin is important in maintaining the integrity of neurons, therefore its disorganization and downregulation would ultimately cause neuronal degeneration that may account for the pathology of *dt* mice.

Interactions of BPAG1 with NFs: Potential Role in the dt Pathogenesis

We have demonstrated in the two-hybrid assays and overlay studies that the COOH-terminal domain of BPAG1 does not interact with wild-type NFTPs. Furthermore, mBPAG-C1 and mBPAG-C2 do not colocalize with the filaments formed by transfected NF-L/NF-M or NF-L/NF-H. However, we cannot exclude the possibility that full-length BPAG1-n can associate with native NFs in axons under normal physiological conditions. Although the tail domains of NFTPs appeared to prevent the proteins from binding to mBPAG-C1 in vitro, it is possible that post-translational modifications of NFTPs and the presence of other linker proteins may expose the BPAG1-binding domain of NFTPs on the surface of NFs in axons, thereby allowing interactions between BPAG1-n and NFTPs. Furthermore, peripherin has been shown to copolymerize with NFTPs (Parysek et al., 1991) and therefore interactions between BPAG1-n with NFTPs could occur indirectly through peripherin.

During the initial phase of *dt* pathogenesis, most of the motoneurons in the BPAG1-deficient mice look normal, indicating that BPAG1 is not necessary for the initial organization of NFs in motoneurons (Duchen and Strich, 1964; Janota, 1972; Duchen, 1976; al-Ali and al-Zuhair, 1989). To study the role of axonal NFs on the pathogenesis of *dt* axonopathy, Eyer et al. (1998) produced homozygous *dt* mice carrying a NFH-lacZ transgene. Because of the impairment in the axonal transport of NFs, these transgenic mice contain sensory neurons with axons devoid of NFs. Neuronal degeneration is still observed in these mice even though very few, if any, axonal swellings (devoid of NFs) are present, suggesting that abnormal accumulations of NFs in axonal swellings are not the only factor in *dt* pathogenesis. Nevertheless, the double transgenic mice displayed a longer life span, indicating that axonal swellings with neurofilamentous accumulations play a secondary role in promoting the neuronal degeneration in *dt* mice. However, it is not yet known whether the abnormal accumulations of NFs in the axons are directly caused by the absence of BPAG1-n, disorganization and downregulation of peripherin, or by the impairment of axonal transport.

The Functions of BPAG1-n and Peripherin: A Lesson from Plectin

Why would peripherin need to be "organized" by BPAG1-n? What causes the downregulation of peripherin in *dt* mice? Why does the *dt* pathology occur late in develop-

ment, even though peripherin and BPAG1-n are expressed early in differentiated neurons? These are some of the questions that remain unanswered. Before we are able to answer these questions, we must first understand the functions of BPAG1-n and peripherin. BPAG1-n is structurally very similar to plectin, although it has a shorter tail domain (Ruhrberg and Watt, 1997). Plectin is known for its ability to associate with many cytoplasmic structures, including IFs, actin filaments, microtubules, myosin filaments, and membrane proteins (Pytela and Wiche, 1980; Svitkina et al., 1996; Wiche, 1998). It is possible that BPAG1-n also interacts with some of these components in neurons. Therefore, perturbations of BPAG1-n may not only affect microfilaments and peripherin, but also other neuronal structures. Until we have identified all the interaction partners of BPAG1-n, it will be difficult to determine the precise cause of the neuronal degeneration in *dt* mice. The function of peripherin is even less understood. Peripherin has been suggested to have a different function than NFTPs, since it is upregulated after nerve injury, while the NFTPs are downregulated (Troy et al., 1990b; Belecky-Adams et al., 1993). However, downregulation of peripherin by antisense oligonucleotides in cultured PC12 cells did not result in any observable effects on process outgrowth (Troy et al., 1992). Nevertheless, our present study shows that BPAG1-n is able to bind peripherin and that the association of BPAG1-n with peripherin appears to have physiological significance and may contribute to the development of *dt* pathology.

We thank Ms. Beth Rosen for technical assistance, Ms. Theresa Swayne for the help with the confocal microscopy, Dr. Gee Ching for editorial assistance, and Dr. Chung-Liang Ho for the preparation of the original peripherin two-hybrid constructs.

This work was supported by grant NS15182 from the National Institutes of Health. C.L. Leung and D. Sun were supported as trainees on training grant AG00189.

Received for publication 8 May 1998 and in revised form 23 December 1998.

References

al-Ali, S.Y., and A.G. al-Zuhair. 1989. Fine structural study of the spinal cord and spinal ganglia in mice afflicted with a hereditary sensory neuropathy, dystonia musculorum. *J. Submicrosc. Cytol. Pathol.* 21:737–748.

Aletta, J.M., R. Angeletti, R.K. Liem, C. Purcell, M.L. Shelanski, and L.A. Greene. 1988. Relationship between the nerve growth factor-regulated clone 73 gene product and the 58-kilodalton neuronal intermediate filament protein (peripherin). *J. Neurochem.* 51:1317–1320.

Amagai, M., T. Hashimoto, S. Tajima, Y. Inokuchi, N. Shimizu, M. Saito, K. Miki, and T. Nishikawa. 1990. Partial cDNA cloning of the 230-kD mouse bullous pemphigoid antigen by use of a human monoclonal anti-basement membrane zone antibody. *J. Invest. Dermatol.* 95:252–259.

Belecky-Adams, T., D.C. Wight, J.J. Kopchick, and L.M. Parysek. 1993. Intragenic sequences are required for cell type-specific and injury-induced expression of the rat peripherin gene. *J. Neurosci.* 13:5056–5065.

Bernier, G., A. Brown, G. Dalpe, Y. De Repentigny, M. Mathieu, and R. Kothary. 1995. Dystonin expression in the developing nervous system predominates in the neurons that degenerate in dystonia musculorum mutant mice. *Mol. Cell. Neurosci.* 6:509–520.

Bousquet, O., and P.A. Coulombe. 1996. Cytoskeleton: missing links found? *Curr. Biol.* 6:1563–1566.

Brody, B.A., C.A. Ley, and L.M. Parysek. 1989. Selective distribution of the 57 kD neural intermediate filament protein in the rat CNS. *J. Neurosci.* 9:2391–2401.

Brown, A., G. Bernier, M. Mathieu, J. Rossant, and R. Kothary. 1995a. The mouse dystonia musculorum gene is a neural isoform of bullous pemphigoid antigen 1. *Nat. Genet.* 10:301–306.

Brown, A., G. Dalpe, M. Mathieu, and R. Kothary. 1995b. Cloning and characterization of the neural isoforms of human dystonin. *Genomics.* 29:777–780.

Chin, S.S., and R.K. Liem. 1989. Expression of rat neurofilament proteins NF-L and NF-M in transfected non-neuronal cells. *Eur. J. Cell. Biol.* 50:475–490.

Chin, S.S., and R.K. Liem. 1990. Transfected rat high-molecular-weight neurofilament (NF-H) coassembles with vimentin in a predominantly nonphosphorylated form. *J. Neurosci.* 10:3714–3726.

Chin, S.S., P. Macioce, and R.K. Liem. 1991. Effects of truncated neurofilament proteins on the endogenous intermediate filaments in transfected fibroblasts. *J. Cell Sci.* 99:335–350.

Ching, G.Y., and R.K. Liem. 1993. Assembly of type IV neuronal intermediate filaments in nonneuronal cells in the absence of preexisting cytoplasmic intermediate filaments. *J. Cell Biol.* 122:1323–1335.

Ching, G., and R. Liem. 1998. Roles of head and tail domains in (alpha)-internexin's self-assembly and coassembly with the neurofilament triplet proteins. *J. Cell Sci.* 111:321–333.

Dowling, J., Q.C. Yu, and E. Fuchs. 1996. Beta4 integrin is required for hemidesmosome formation, cell adhesion and cell survival. *J. Cell Biol.* 134: 559–572.

Dowling, J., Y. Yang, R. Wollmann, L.F. Reichardt, and E. Fuchs. 1997. Developmental expression of BPAG1-n: insights into the spastic ataxia and gross neurologic degeneration in dystonia musculorum mice. *Dev. Biol.* 187:131–142.

Duchen, L.W. 1976. Dystonia musculorum: an inherited disease of the nervous system in the mouse. *Adv. Neurol.* 14:353–365.

Duchen, L.W., and S.J. Strich. 1964. Clinical and pathological studies of an hereditary neuropathy in mice (*dystonia musculorum*). *Brain.* 87:367–378.

Duchen, L.W., D.S. Falconer, and S.J. Strich. 1963. Dystonia musculorum. A hereditary neuropathy of mice affecting mainly sensory pathway. *J. Physiol.* 165:7–9.

Errante, L.D., G. Wiche, and G. Shaw. 1994. Distribution of plectin, an intermediate filament-associated protein, in the adult rat central nervous system. *J. Neurosci. Res.* 37:515–528.

Escurat, M., K. Djabali, M. Gumpel, F. Gros, and M.M. Portier. 1990. Differential expression of two neuronal intermediate-filament proteins, peripherin and the low-molecular-mass neurofilament protein (NF-L), during the development of the rat. *J. Neurosci.* 10:764–784.

Eyer, J., D.W. Cleveland, P.C. Wong, and A.C. Peterson. 1998. Pathogenesis of two axonopathies does not require axonal neurofilaments. *Nature.* 391:584–587.

Fliegner, K.H., and R.K. Liem. 1991. Cellular and molecular biology of neuronal intermediate filaments. *Int. Rev. Cytol.* 131:109–167.

Fliegner, K.H., M.P. Kaplan, T.L. Wood, J.E. Pintar, and R.K. Liem. 1994. Expression of the gene for the neuronal intermediate filament protein alpha-internexin coincides with the onset of neuronal differentiation in the developing rat nervous system. *J. Comp. Neurol.* 342:161–173.

Fuchs, E., and D.W. Cleveland. 1998. A structural scaffolding of intermediate filaments in health and disease. *Science.* 279:514–519.

Green, K.J., M.L.A. Virata, G.W. Elgart, J.R. Stanley, and D.A.D. Parry. 1992. Comparative structural analysis of desmoplakin, bullous pemphigoid antigen and plectin: members of a new gene family involved in organization of intermediate filaments. *Int. J. Biol. Macromol.* 14:145–153.

Guo, L., L. Degenstein, J. Dowling, Q.C. Yu, R. Wollmann, B. Perman, and E. Fuchs. 1995. Gene targeting of BPAG1: abnormalities in mechanical strength and cell migration in stratified epithelia and neurologic degeneration. *Cell.* 81:233–243.

Ho, C.L., and R.K. Liem. 1996. Intermediate filaments in the nervous system: implications in cancer. *Cancer Metastasis Rev.* 15:483–497.

Ho, C.L., S.S. Chin, K. Carnevale, and R.K. Liem. 1995. Translation initiation and assembly of peripherin in cultured cells. *Eur. J. Cell Biol.* 68:103–112.

Houseweart, M.K., and D.W. Cleveland. 1998. Intermediate filaments and their associated proteins: multiple dynamic personalities. *Curr. Opin. Cell Biol.* 10:93–101.

Janota, I. 1972. Ultrastructural studies of an hereditary sensory neuropathy in mice (dystonia musculorum). *Brain.* 95:529–536.

Kaplan, M.P., S.S. Chin, K.H. Fliegner, and R.K. Liem. 1990. Alpha-internexin, a novel neuronal intermediate filament protein, precedes the low molecular weight neurofilament protein (NF-L) in the developing rat brain. *J. Neurosci.* 10:2735–2748.

Kaplan, M.P., S.S. Chin, P. Macioce, J. Srinawasan, G. Hashim, and R.K. Liem. 1991. Characterization of a panel of neurofilament antibodies recognizing N-terminal epitopes. *J. Neurosci. Res.* 30:545–554.

Lee, M.K., and D.W. Cleveland. 1996. Neuronal intermediate filaments. *Annu. Rev. Neurosci.* 19:187–217.

Lee, M.K., Z. Xu, P.C. Wong, and D.W. Cleveland. 1993. Neurofilaments are obligate heteropolymers in vivo. *J. Cell Biol.* 122:1337–1350.

Leonard, D.G., J.D. Gorham, P. Cole, L.A. Greene, and E.B. Ziff. 1988. A nerve growth factor-regulated messenger RNA encodes a new intermediate filament protein. *J. Cell Biol.* 106:181–193.

Leung, C.L., and R.K.H. Liem. 1996. Characterization of interactions between the neurofilament triplet proteins by the yeast two-hybrid system. *J. Biol. Chem.* 271:14041–14044.

Lieber, J.G., and R.M. Evans. 1996. Disruption of the vimentin intermediate filament system during adipose conversion of 3T3-L1 cells inhibits lipid droplet accumulation. *J. Cell Sci.* 109:3047–3058.

Liem, R.K.H., and S.B. Hutchison. 1982. Purification of the individual components of the neurofilament triplet: filament assembly from the 70,000 dalton subunit. *Biochemistry.* 21:3221–3226.

Meng, J.J., E.A. Bornslaeger, K.J. Green, P.M. Steinert, and W. Ip. 1997. Two-hybrid analysis reveals fundamental differences in direct interactions be-

tween desmoplakin and cell type-specific intermediate filaments. *J. Biol. Chem.* 272:21495–21503.
Mueller, S., V. Klaus-Kovtun, and J.R. Stanley. 1989. A 230-kD basic protein is the major bullous pemphigoid antigen. *J. Invest. Dermatol.* 92:33–38.
Napolitano, E.W., S.S. Chin, D.R. Colman, and R.K.H. Liem. 1987. Complete amino acid sequence and in vitro expression of rat NF-M, the middle molecular weight neurofilament protein. *J. Neurosci.* 7:2590–2599.
Nikolic, B., E.M. Nulty, D.B. Mir, and G. Wiche. 1996. Basic amino acid residue cluster within nuclear targeting sequence motif is essential for cytoplasmic plectin-vimentin network junctions. *J. Cell Biol.* 134:1455–1467.
Pachter, J.S., and R.K. Liem. 1984. The differential appearance of neurofilament triplet polypeptides in the developing rat optic nerve. *Dev. Biol.* 103: 200–210.
Parysek, L.M., and R.D. Goldman. 1988. Distribution of a novel 57 kD intermediate filament (IF) protein in the nervous system. *J. Neurosci.* 8:555–563.
Parysek, L.M., R.L. Chisholm, C.A. Ley, and R.D. Goldman. 1988. A type III intermediate filament gene is expressed in mature neurons. *Neuron.* 1:395–401.
Parysek, L.M., M.A. McReynolds, R.D. Goldman, and C.A. Ley. 1991. Some neural intermediate filaments contain both peripherin and the neurofilament proteins. *J. Neurosci. Res.* 30:80–91.
Pytela, R., and G. Wiche. 1980. High molecular weight polypeptides (270,000–340,000) from cultured cells are related to hog brain microtubule-associated proteins but copurify with intermediate filaments. *Proc. Natl. Acad. Sci. USA.* 77:4808–4812.
Ruhrberg, C., and F.M. Watt. 1997. The plakin family: versatile organizers of cytoskeletal architecture. *Curr. Opin. Genet. Dev.* 7:392–397.
Ruhrberg, C., M.A. Hajibagheri, D.A. Parry, and F.M. Watt. 1997. Periplakin, a novel component of cornified envelopes and desmosomes that belongs to the plakin family and forms complexes with envoplakin. *J. Cell Biol.* 139: 1835–1849.
Shaw, G., and K. Weber. 1982. Differential expression of neurofilament triplet proteins in brain development. *Nature.* 298:277–279.
Sotelo, C., and J.L. Guenet. 1988. Pathologic changes in the CNS of dystonia musculorum mutant mouse: an animal model for human spinocerebellar ataxia. *Neuroscience.* 27:403–424.
Stanley, J.R. 1993. Cell adhesion molecules as targets of autoantibodies in pemphigus and pemphigoid, bullous diseases due to defective epidermal cell adhesion. *Adv. Immunol.* 53:291–325.
Stanley, J.R., T. Tanaka, S. Mueller, V. Klaus-Kovtun, and D. Roop. 1988. Isolation of complementary DNA for bullous pemphigoid antigen by use of patients' autoantibodies. *J. Clin. Invest.* 82:1864–1870.
Sun, D., P. Macioce, S.S. Chin, and R.K. Liem. 1997. Assembly properties of amino- and carboxyl-terminally truncated neurofilament NF-H proteins with NF-L and NF-M in the presence and absence of vimentin. *J. Neurochem.* 68:917–926.
Svitkina, T.M., A.B. Verkhovsky, and G.G. Borisy. 1996. Plectin sidearms mediate interaction of intermediate filaments with microtubules and other components of the cytoskeleton. *J. Cell Biol.* 135:991–1007.
Troy, C.M., K. Brown, L.A. Greene, and M.L. Shelanski. 1990a. Ontogeny of the neuronal intermediate filament protein, peripherin, in the mouse embryo. *Neuroscience.* 36:217–237.
Troy, C.M., N.A. Muma, L.A. Greene, D.L. Price, and M.L. Shelanski. 1990b. Regulation of peripherin and neurofilament expression in regenerating rat motor neurons. *Brain Res.* 529:232–238.
Troy, C.M., L.A. Greene, and M.L. Shelanski. 1992. Neurite outgrowth in peripherin-depleted PC12 cells. *J. Cell Biol.* 117:1085–1092.
Wiche, G. 1998. Role of plectin in cytoskeleton organization and dynamics. *J. Cell Sci.* 111:2477–2486.
Yang, Y., J. Dowling, Q.C. Yu, P. Kouklis, D.W. Cleveland, and E. Fuchs. 1996. An essential cytoskeletal linker protein connecting actin microfilaments to intermediate filaments. *Cell.* 86:655–665.